An exact matrix calculation for a two-dimensional model of the steam-water-ice system: bulk and boundary properties

1976 J. Phys. A: Math. Gen. 9 2077

(http://iopscience.iop.org/0305-4470/9/12/013)

J. Phys. A: Math. Gen., Vol. 9, No. 12, 1976. Printed in Great Britain.

An exact matrix calculation for a two-dimensional model of the steam–water–ice system: bulk and boundary properties

D A Lavis

Mathematics Department, Chelsea College, University of London, Manresa Road, London SW3 6LX, UK

Received 7 April 1976, in final form 28 June 1976

Abstract. The model studied consists of a two-dimensional triangular lattice of which some sites are occupied by the centres of molecules, the remainder being unoccupied. Each molecule has three bonding directions at angles of 120° to each other and two possible orientations, in each of which its bonding directions point to three of the six nearest-neighbour sites. If the molecules of a nearest-neighbour pair have bonding directions pointing towards each other a bond is formed; bonded and unbonded pairs have different interaction energies.

The lattice is wrapped around a semi-infinite cylinder terminating in a row of boundary sites. This allows an exact matrix calculation to be performed. Maxima of the isothermal compressibility are located and it is shown that these maxima become steeper as the width of the lattice increases. The 'phase diagram' of these maxima is compared with the corresponding phase diagram obtained from the author's first-order calculations. The probabilities for different types of occupation of the boundary sites are determined by the interaction with the environment and the successive occupations of the sites of the lattice, proceeding in a direction away from the boundary, are given by a stationary Markov chain. It is shown by computer calculations that the local molecular number density and the probability of site occupation by a monomer both fluctuate in a damped periodic way.

1. Introduction

Since the work of Bernal and Fowler (1933) it has been widely recognized that many of the 'anomalous' properties of water arise from the existence of regions of open structure with a lower density than other molecular arrangements (see, e.g., Eisenberg and Kauzmann 1969, Fletcher 1970, Perram and Levine 1974). This point of view has recently been embodied in one-dimensional (Bell 1969, Bell and Salt 1973), two-dimensional (Bell and Lavis 1970a, b, Lavis 1973, 1975) and three-dimensional (Perram 1971, Bell 1972, Bell and Sallouta 1975, Bell and Salt 1976) lattice theories. This work supports the contention that the competition between molecular order of open and close-packed forms leads to water-like behaviour.

In the two papers of Bell and Lavis (1970a, b) a two-dimensional triangular lattice model was considered in which the molecules form bonds in such a way that an open honeycomb structure with vacant sites is necessary for all molecules to be fully bonded. The model of Bell and Lavis (1970a) is of the interstitial type. The low temperature open honeycomb configuration is ensured by an initial choice of a honeycomb array and molecules are allowed to bond only when they occupy neighbouring sites on this array.

In this model the liquid state corresponds to a form of long-range ordering between the honeycomb array and the remaining interstitial sites. Since order in the liquid state is generally regarded as short-range in character this approach is not very satisfactory. In the second paper (Bell and Lavis 1970b) a model was developed for the liquid and vapour states in which the open structure is a form of short-range ordering. Using a first-order approximation based on a triangle of sites, one phase transition of the steam–water type was obtained, together with the characteristic density maximum found in water. Lavis (1975) investigated the symmetry properties of this model and, using these properties, obtained a simple equation for the coexistence curve. This allowed a detailed examination of the thermodynamic response functions along this curve. Water-like behaviour is again observed. The extension of this model to include a long-range ordered phase is given by Lavis (1973). The long-range ordered phase can be identified as a solid phase which occurs by a transition of the water–ice type from the liquid phase.

In the present work we study the model of Bell and Lavis (1970b) and Lavis (1973, 1975) but, instead of choosing a two-dimensionally infinite assembly, we consider a lattice in the form of $2n$ rows, each of N sites, wrapped around a cylinder. The form of the lattice is shown in figure 1, the first and $(2n+1)$th rows being coincident on the surface of a cylinder. In order to be able to include a study of boundary effects, the thermodynamic limit is taken by projecting one end of the cylinder to infinity. Models of this kind have been studied extensively, using the matrix method, for assemblies of hard molecules (see, e.g., Ree and Chesnut 1966, Runnels and Combs 1966, Runnels *et al* 1967, Bellemans and Nigam 1967, Orban and Bellemans 1968, Orban *et al* 1968).

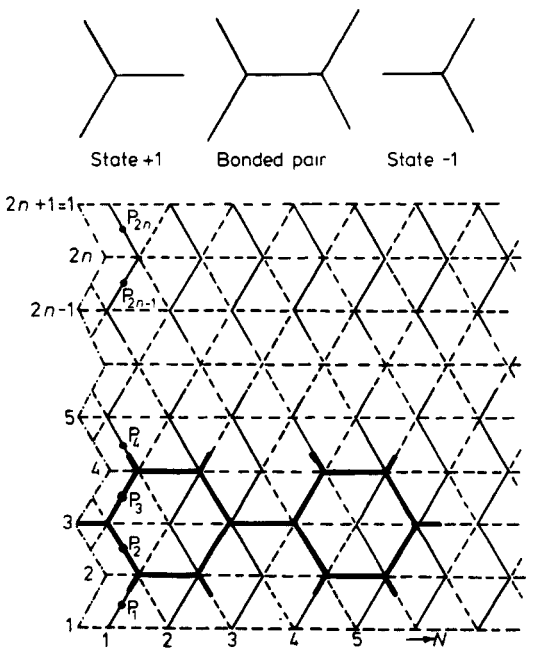

Figure 1. Orientational states of molecules and the left-hand end of the lattice. Elements of the lattice are represented by a full line and a fragment of the honeycomb fully-bonded structure is given by a bold full line.

Although no phase transitions occur, maxima in the compressibility can be regarded as 'incipient phase transitions'. This question is further discussed in § 4.

The main advantage of this method is that it is exact. It will therefore, in our case, provide a comparison with the first-order approximation work of Bell and Lavis (1970b) and Lavis (1973). A second advantage of this method is that it facilitates the investigation of boundary effects. From a theoretical point of view a study of these effects for two- or three-dimensional lattice models presents considerable difficulties. (For a survey of work on surface effects in Ising models see Watson (1972).) It has however been shown by the work of Bell and Salt (1973) that these properties can be effectively considered, for a system with a low-energy open structure, if a suitable one-dimensional model is chosen. In this context, a 'one-dimensional model' can be understood to be any planar model which is only one-dimensionally infinite. Boundary effects are of some importance for the water system. In particular it is interesting to know, within the context of the model, if the disturbance due to the interface of water with another medium has any long-range effects on the water structure. The experimental work of Clifford *et al* (1970), using nuclear magnetic resonance measurements, led to the conclusion that, for the surfaces examined, there were no long-range effects. This result is in agreement with the theoretical studies of Bell and Salt (1973). The present work provides an additional investigation of these effects.

2. The lattice model

Each site of the lattice will either be occupied by a molecule or it will be vacant (be occupied by a 'hole') and each molecule possesses three bonding directions at 120° to each other. A molecule on a lattice site has two orientational states labelled '-1' and '$+1$' (see figure 1) in each of which it has bonding directions pointing towards three of the six neighbouring sites. Since molecular bonding is intended, in this model, to represent in a simple way the hydrogen bonding between water molecules, we allow a bond to form between neighbouring molecules if and only if bonding directions from each member of the pair point towards each other. The interaction energy of the pair is in this case $-(\epsilon+w)$ with $\epsilon \geqslant 0$ and $w>0$. In all other cases of a pair of molecules occupying neighbouring sites no bond can be formed and the interaction energy is $-\epsilon$. Interaction energies between molecules which do not occupy neighbouring sites are neglected.

The lattice can be regarded as composed of N 'elements', each element consisting of $2n$ sites forming a zig-zag ring of nearest neighbour sites around the cylinder on which the lattice is situated (see figure 1). There will be 3^{2n} ways of occupying the sites of an element of the lattice. Labelling the state of an unoccupied site by '0', we may represent the occupational state of an element of the lattice by a vector $\boldsymbol{\eta} = (s_{2n}, s_{2n-1}, \ldots, s_1)$†, where $s_j = -1, 0$ or $+1$, for $j = 1, 2, \ldots, 2n$. The interaction energy E_η within an element of the lattice with occupational state $\boldsymbol{\eta}$ is given by

$$E_\eta = -\tfrac{1}{4} \sum_{j=1}^{n} (\phi(w, \epsilon; s_{2j}, s_{2j-1}) + \phi(w, \epsilon; s_{2j}, s_{2j+1})) \tag{2.1}$$

† Notation: throughout this work lower case Greek or Latin letters in bold italic will represent row vectors; sans serif bold upper case letters will represent matrices. The superscript asterisk will indicate the Hermitian adjoint of a matrix (or vector). The Hermitian adjoint of a matrix of real elements is its transpose; the Hermitian adjoint of a row vector of real elements is the corresponding column vector.

where the indices, in this and subsequent equations, are taken to be integers modulo $2n$ and

$$\phi(w, \epsilon; x, y) = xy[w(x+1)(y-1)+4\epsilon xy] = \phi(w, \epsilon; -y, -x). \tag{2.2}$$

Suppose that the right-hand neighbour of this element has occupational state $\boldsymbol{\xi} = (s'_{2n}, s'_{2n-1}, \ldots, s'_1)$, then the interaction energy $E_{\eta\xi}$ between these two elements of the lattice is given by

$$E_{\eta\xi} = -\tfrac{1}{4}\sum_{j=1}^{n} (\phi(w, \epsilon; s'_{2j-1}, s_{2j}) + \phi(w, \epsilon; s_{2j}, s'_{2j}) + \phi(w, \epsilon; s'_{2j+1}, s_{2j}) + \tfrac{1}{2}\phi(w, \epsilon; s_{2j+1}, s'_{2j+1}) + \tfrac{1}{2}\phi(w, \epsilon; s_{2j-1}, s'_{2j-1})). \tag{2.3}$$

Let the chemical potential of each molecule be μ, then the chemical potential associated with the occupational state $\boldsymbol{\eta}$ is

$$\mu_\eta = \sum_{j=1}^{2n} \mu s_j^2. \tag{2.4}$$

We shall suppose that the system is in thermal and chemical equilibrium with its environment and in mechanical isolation. The independent variables of the system are the absolute temperature T, the molecular chemical potential μ and the lattice volume $2nNA_0$, where A_0 is the (two-dimensional) lattice volume per site. The dependent variables are the entropy S, the number of molecules M and the pressure P. (Supposing that the boundaries of the lattice follow the zig-zag shape of the lattice elements and are situated at half the nearest-neighbour distance to the left of the first element and to the right of the Nth element (see figure 1), it follows that the triangle formed by three nearest-neighbour sites has area $A_0/2$.) For thermodynamic stability the thermodynamic potential D is a minimum, where D is given by

$$D = U - ST - \mu M, \tag{2.5}$$

where U is the internal energy of the system. Suppose that for fixed chemical potential and lattice volume the temperature of the system is reduced to absolute zero. If the system tends to the completely ordered honeycomb arrangement of molecules the number of molecules tends to $4nN/3$, each molecule being fully bonded to three of its nearest neighbours. The molecular arrangement can be represented by the transposed occupation vectors:

$$\ldots \begin{pmatrix} +1 \\ -1 \\ \vdots \\ +1 \\ -1 \\ +1 \\ -1 \end{pmatrix} \begin{pmatrix} -1 \\ 0 \\ \vdots \\ -1 \\ 0 \\ -1 \\ 0 \end{pmatrix} \begin{pmatrix} 0 \\ +1 \\ \vdots \\ 0 \\ +1 \\ 0 \\ +1 \end{pmatrix} \begin{pmatrix} +1 \\ -1 \\ \vdots \\ +1 \\ -1 \\ +1 \\ -1 \end{pmatrix} \begin{pmatrix} -1 \\ 0 \\ \vdots \\ -1 \\ 0 \\ -1 \\ 0 \end{pmatrix} \ldots$$

For large N the interaction with the boundaries becomes negligible, the internal energy tends to $-2nN(\epsilon+w)$ and D tends to $D^{(0)}$ given by

$$D^{(0)} = -2nN(3\epsilon+3w+2\mu)/3. \tag{2.6a}$$

The alternative to this arrangement is for all sites of the lattice to be occupied as the temperature tends to absolute zero. In this case the minimum internal energy is achieved with each molecule bonding on average with two neighbouring molecules. There is a large number of different ways of achieving this state, e.g.:

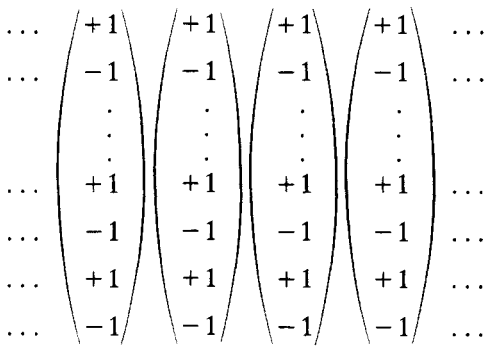

the degeneracy of the state being the same as that of the triangular Ising antiferromagnet (see Bell and Lavis 1970b, appendix). In this case the internal energy tends to $-2nN(3\epsilon+w)$ and D tends to $D^{(c)}$ given by

$$D^{(c)} = -2nN(3\epsilon+w+\mu). \tag{2.6b}$$

From the condition for thermodynamic stability we see that the system attains the open or close-packed state, as the temperature tends to absolute zero, at constant chemical potential, according as μ is less than or greater than $\mu_0 = -6\epsilon$. Now at thermodynamic equilibrium

$$D = -2nNA_0P \tag{2.7}$$

and it follows from equations (2.6*a*) and (2.7) that, as the temperature tends to absolute zero along a curve of constant chemical potential, a positive value of pressure will be attained if and only if

$$\mu > -3(\epsilon+w)/2. \tag{2.8}$$

Corresponding to the chemical potential μ_0 we have

$$D_0 = -2nNA_0P_0 = -2nN(w-3\epsilon), \tag{2.9}$$

where P_0 is the separation pressure derived by Bell and Lavis (1970a) for a system which is in thermal and mechanical equilibrium with its environment but in chemical isolation. It is clear that if $\mu < \mu_0$ then the limiting value for the pressure must be less than P_0. Thus, in order for the open structure to be a possible stable equilibrium state, as the temperature tends to absolute zero, we must have

$$P_0 = (w-3\epsilon)/A_0 > 0. \tag{2.10}$$

3. The matrix method

The distribution appropriate to a system in thermal and chemical equilibrium with its environment and in mechanical isolation is the grand canonical distribution for which

$$D = -kT \ln \Xi(\mu, N, T) \tag{3.1}$$

where Ξ is the grand canonical partition function and k is Boltzmann's constant. From equations (2.7) and (3.1) the pressure P of the system is given by

$$\left(\frac{PA_0}{w}\right) = \left(\frac{kT}{w}\right)\left(\frac{1}{2nN} \ln \Xi(\mu, N, T)\right). \tag{3.2}$$

The 3^{2n} occupational states of an element of the lattice are ordered according to the symmetry properties described in the appendix† and we construct the $3^{2n} \times 3^{2n}$ dimensional matrix

$$\mathbf{V} = (\exp(\tfrac{1}{2}\mu_\eta - \tfrac{1}{2}E_\eta - E_{\eta\xi} - \tfrac{1}{2}E_\xi + \tfrac{1}{2}\mu_\xi)/kT). \tag{3.3}$$

With respect to the representation R of the dihedral group we have (see appendix, equations (A.1), (A.2))

$$\mathbf{R}(C_n^{(s)})\mathbf{V}\mathbf{R}(C_n^{(s)}) = \mathbf{V} \tag{3.4a}$$

$$\mathbf{R}(\sigma_s)\mathbf{V}\mathbf{R}(\sigma_s) = \mathbf{V} \tag{3.4b}$$

for $s = 1, 2, \ldots, n$ and

$$\mathbf{R}(U_2^{(1)})\mathbf{V}\mathbf{R}(U_2^{(1)}) = \mathbf{V}^*. \tag{3.4c}$$

If the first (left-hand end) element of the lattice has occupational state $\boldsymbol{\eta}$ we suppose that it interacts with the boundary with energy $E_\eta^{(L)}$ and if the Nth (right-hand end) element has this occupation state we suppose that it interacts with the boundary with energy $E_\eta^{(R)}$. In terms of these energies we define the 3^{2n}-dimensional vectors

$$\boldsymbol{\alpha} = (\exp[-(E_\eta^{(L)} - \tfrac{1}{2}\mu_\eta + \tfrac{1}{2}E_\eta)/kT]) \tag{3.5a}$$

and

$$\boldsymbol{\beta} = (\exp[-(\tfrac{1}{2}E_\eta - \tfrac{1}{2}\mu_\eta + E_\eta^{(R)})/kT]). \tag{3.5b}$$

We shall suppose that

$$\mathbf{R}(C_n^{(s)})\boldsymbol{\alpha}^* = \boldsymbol{\alpha}^* \qquad \mathbf{R}(C_n^{(s)})\boldsymbol{\beta}^* = \boldsymbol{\beta}^* \tag{3.6a}$$

$$\mathbf{R}(\sigma_s)\boldsymbol{\alpha}^* = \boldsymbol{\alpha}^* \qquad \mathbf{R}(\sigma_s)\boldsymbol{\beta}^* = \boldsymbol{\beta}^* \tag{3.6b}$$

for $s = 1, 2, \ldots, n$ and

$$\mathbf{R}(U_2^{(1)})\boldsymbol{\alpha}^* = \boldsymbol{\beta}^* \qquad \mathbf{R}(U_2^{(1)})\boldsymbol{\beta}^* = \boldsymbol{\alpha}^*. \tag{3.6c}$$

This is equivalent to assuming that the system has identical interactions with its two boundaries, these interactions being invariant under any operation of the group $\mathscr{C}_{nv}$.

It may be shown (see, e.g., Bell and Salt 1973) that

$$\Xi(\mu, N, T) = \boldsymbol{\alpha}\mathbf{V}^{N-1}\boldsymbol{\beta}^*. \tag{3.7}$$

† The appendix contains only a brief description of the dihedral group. Its multiplication table, together with a representation R of the group for $n = 1$ and 2, is contained in another unpublished appendix which can be obtained by writing to the author.

The probability $p_\eta(i)$ that the ith element has occupation $\boldsymbol{\eta}$ for $1 \leqslant i \leqslant N$ is given, in terms of the vector $\hat{\boldsymbol{\imath}}_\eta$ defined in the appendix, by

$$p_\eta(i) = \frac{(\boldsymbol{\alpha}\mathbf{V}^{i-1}\hat{\boldsymbol{\imath}}_\eta^*)(\hat{\boldsymbol{\imath}}_\eta\mathbf{V}^{N-i}\boldsymbol{\beta}^*)}{\boldsymbol{\alpha}\mathbf{V}^{N-1}\boldsymbol{\beta}^*} \tag{3.8}$$

and the conditional probability $p_{\eta\xi}(i, k)$ that the kth element has occupation $\boldsymbol{\xi}$ given that the ith element has occupation $\boldsymbol{\eta}$ for $1 \leqslant i \leqslant k \leqslant N$ is given by

$$p_{\eta\xi}(i, k) = \frac{(\hat{\boldsymbol{\imath}}_\eta\mathbf{V}^{k-i}\hat{\boldsymbol{\imath}}_\xi^*)(\hat{\boldsymbol{\imath}}_\xi\mathbf{V}^{N-k}\boldsymbol{\beta}^*)}{\hat{\boldsymbol{\imath}}_\eta\mathbf{V}^{N-i}\boldsymbol{\beta}^*}. \tag{3.9}$$

It is evident from equation (3.9) that the process of occupation of successive elements of the lattice is a Markov chain with transition probability $p_{\eta\xi}(i-1, i)$ for the ith element to have occupation $\boldsymbol{\xi}$ given that the $(i-1)$th element has occupation $\boldsymbol{\eta}$ (see, e.g., Parzen 1960, p 136).

Let the right eigen-equation for $\mathbf{V}$ be of the form

$$\mathbf{V}\boldsymbol{e}^{(m)*} = \boldsymbol{e}^{(m)*}x_m \qquad m = 1, 2, \ldots, 3^{2n}, \tag{3.10a}$$

where we suppose that the right eigenvalues are, as far as possible, ordered according to decreasing modulus. From equations (3.4*c*) and (3.10*a*)

$$\boldsymbol{d}^{(m)}\mathbf{V} = x_m\boldsymbol{d}^{(m)} \qquad m = 1, 2, \ldots, 3^{2n} \tag{3.10b}$$

where

$$\boldsymbol{d}^{(m)} = \boldsymbol{e}^{(m)}\mathbf{R}(\mathrm{U}_2^{(1)}) \qquad m = 1, 2, \ldots, 3^{2n} \tag{3.11}$$

and

$$\boldsymbol{d}^{(m)}\boldsymbol{e}^{(l)*} = \boldsymbol{e}^{(m)}\mathbf{R}(\mathrm{U}_2^{(1)})\boldsymbol{e}^{(l)*} = \delta_{m,l} \qquad m, l = 1, 2, \ldots, 3^{2n}. \tag{3.12}$$

(For degenerate eigenvalues we can choose an orthonormal basis for the subspace defined by the eigenvalue.) All elements of the matrix $\mathbf{V}$ are strictly greater than zero and it follows from Perron's theorem (see Gantmacher 1959, p 64) that

(i) x_1 is real and positive;
(ii) $x_1 > |x_m|$, $m = 2, 3, \ldots, 3^{2n}$;
(iii) the vector $\boldsymbol{e}^{(1)}$ has real strictly positive elements.

Let $\boldsymbol{\Theta}$ be the diagonal matrix with the elements of $\boldsymbol{e}^{(1)}$ along the diagonal. We construct the matrix

$$\boldsymbol{\Pi} = \boldsymbol{\Theta}^{-1}\mathbf{V}\boldsymbol{\Theta}/x_1. \tag{3.13}$$

This matrix has the eigenvalues $h_m = (x_m/x_1)$ with corresponding right and left eigenvectors

$$\boldsymbol{g}^{(m)} = \boldsymbol{e}^{(m)}\boldsymbol{\Theta}^{-1} = ((e_1^{(m)}/e_1^{(1)}), \ldots, (e_{3^{2n}}^{(m)}/e_{3^{2n}}^{(1)})) \tag{3.14a}$$

and

$$\boldsymbol{q}^{(m)} = \boldsymbol{d}^{(m)}\boldsymbol{\Theta} = ((d_1^{(m)}e_1^{(1)}), \ldots, (d_{3^{2n}}^{(m)}e_{3^{2n}}^{(1)})) \tag{3.14b}$$

respectively for $m = 1, 2, \ldots, 3^{2n}$. Since $h_1 = 1$ and $\boldsymbol{g}^{(1)} = \boldsymbol{j} = (1, 1, 1, \ldots, 1)$ it follows that $\boldsymbol{\Pi}$ is a stochastic matrix. It is not difficult to show that, for any integer $r \geqslant 0$,

$$\boldsymbol{\Pi}^r = \sum_{m=1}^{3^{2n}} h_m^r(\boldsymbol{g}^{(m)*} \otimes \boldsymbol{q}^{(m)}), \tag{3.15}$$

where $\mathbf{\Pi}^0$ is taken to be the unit matrix. For small values of r this equation is of no great importance since powers of $\mathbf{\Pi}$ can be calculated by matrix multiplication. It does however become significant in the limit of large r where, since $|h_m|<1$ for $m>1$, we have

$$\mathbf{\Pi}^r \sim \boldsymbol{j}^* \otimes \boldsymbol{q}^{(1)}. \tag{3.16}$$

We shall in this work be concerned with the thermodynamic limit, $N \to \infty$. Substituting from equations (3.13)–(3.16) into (3.2) and (3.7)–(3.9) we have

$$\left(\frac{PA_0}{w}\right) \sim \left(\frac{kT}{w}\right)\left(\frac{1}{2n}\ln x_1 + \frac{1}{2nN}\ln[(\boldsymbol{\alpha e}^{(1)*})(\boldsymbol{d}^{(1)}\boldsymbol{\beta}^*)]\right) \sim \left(\frac{kT}{w}\right)\left(\frac{\ln x_1}{2n}\right) \tag{3.17a}$$

$$p_\eta(i) \sim \frac{(\boldsymbol{\alpha\Theta\Pi}^{i-1}\boldsymbol{\Theta}^{-1}\hat{\boldsymbol{i}}_\eta^*)(\hat{\boldsymbol{i}}_\eta \boldsymbol{e}^{(1)*})}{\boldsymbol{\alpha e}^{(1)*}} = \left(\frac{\boldsymbol{\alpha\Theta}}{\boldsymbol{\alpha e}^{(1)*}}\right)\mathbf{\Pi}^{i-1}\hat{\boldsymbol{i}}_\eta^* \tag{3.17b}$$

and

$$p_{\eta\xi}(i, k) \sim \hat{\boldsymbol{i}}_\eta \mathbf{\Pi}^{k-i}\hat{\boldsymbol{i}}_\xi^* = \Pi_{\eta\xi}^{(k-i)}, \tag{3.17c}$$

where $\Pi_{\eta\xi}^{(r)}$ is the η–ξ element of $\mathbf{\Pi}^r$.

We see that in the thermodynamic limit the Markov chain of occupational probabilities is homogeneous with transition matrix $\mathbf{\Pi}$. The initial probability vector $\boldsymbol{p}(1)$ is given by

$$\boldsymbol{p}(1) = \boldsymbol{\alpha\Theta}/\boldsymbol{\alpha e}^{(1)*} \tag{3.18}$$

and the probability vector for the rth element is

$$\boldsymbol{p}(r) = \boldsymbol{p}(1)\mathbf{\Pi}^{r-1}. \tag{3.19}$$

From equations (3.16) and (3.19)

$$\lim_{r\to\infty} \boldsymbol{p}(r) = \boldsymbol{p}(1)(\boldsymbol{j}^* \otimes \boldsymbol{q}^{(1)}) = \boldsymbol{q}^{(1)}. \tag{3.20}$$

The vector $\boldsymbol{q}^{(1)}$ is the stationary probability vector for the Markov chain.

4. Bulk properties

The bulk number density $\rho = (M/2nN)$ of molecules on the lattice can, in the thermodynamic limit, be calculated by using either one of the two equivalent equations

$$\rho = \left(\frac{\partial P'}{\partial \mu'}\right)_T \tag{4.1a}$$

and

$$\rho = \frac{1}{2n}\sum_\eta \left(\frac{\mu_\eta}{\mu}\right) q_\eta^{(1)}, \tag{4.1b}$$

where $\mu' = (\mu/w)$ is the reduced chemical potential, the reduced pressure $P' = (PA_0/w)$ is given by equation (3.17a) and the elements of the stationary probability vector $\boldsymbol{q}^{(1)}$ are given by equation (3.14b).

Since the largest eigenvalue x_1 of the matrix $\mathbf{V}$ is non-degenerate (see § 3) the system will undergo no phase transitions (see, e.g., Domb 1960, § 3.2.3). It can however be shown (Ree and Chesnut 1966, § II.D) that, if there exists a function f of μ' such that

$$\lim_{n\to\infty} |h_2(n)|^n = f(\mu') \neq 0, \tag{4.2}$$

then there will, in this limit, be a non-zero correlation between the occupations of widely separated elements of the lattice. Unlike Ree and Chesnut (1966), who, for a system of hard squares, have obtained numerical results for a lattice of up to eighteen rows, we are unable to obtain any reliable idea of whether such a function f exists. This is due to the complexity of our model for which the matrix $\mathbf{V}$ grows in dimension with respect to n according to 3^{2n}. We have found it necessary in our numerical calculations to restrict ourselves to the two cases $n = 1$ and $n = 2$. It is however of some interest to calculate $|h_2(n)|^n$ for these two cases as a function of the reduced chemical potential along isotherms.

The reduced isothermal compressibility $\kappa'_T = (\kappa_T w/A_0)$ of the system is given by

$$\kappa'_T = \frac{1}{\rho^2}\left(\frac{\partial\rho}{\partial\mu'}\right)_T. \tag{4.3}$$

We are considering a system with independent variables $\mu' = (\mu/w)$ and $T' = (kT/w)$. For the two-dimensionally infinite system, corresponding to the limit of large n, we could locate the phase transition curve in the (μ', T') plane by determining the singularities of κ'_T. Intuitively it seems reasonable to identify a maximum in κ'_T, for finite n, with the presence of a phase transition in the two-dimensionally infinite system, provided that the maximum becomes increasingly steep as n is increased. There are however a number of reasons for caution when locating such 'incipient' phase transitions:

(i) Since the singularities in κ'_T, for the infinite system, arise from singularities in $(\partial\rho/\partial\mu')_T$, any function of the form

$$g(i, j, k; \mu', T') = \mu'^i T'^j \rho^k(\mu', T')\kappa'_T(\mu', T'), \tag{4.4}$$

for positive integers i, j and k, would exhibit precisely the same singularities as κ'_T. For finite n however the maxima in the different g's would be located at different points in the (μ', T') plane.

(ii) Given particular values of i, j and k for equation (4.4), it is not necessarily the case that maxima in g as a function of μ' along a curve of constant T' will coincide with those of g as a function of T' along a curve of constant μ'. For the infinite system, the corresponding singularities would coincide.

(iii) The high-density behaviour of a system with n infinite is not immediately obtainable from a system with n finite. This point is well illustrated by Bellemans and Nigam (1967) who obtain series expansions for their model from the matrix method and from high-density series. For the pressure these expansions differ in all but the leading term indicating the possibility of maxima in the compressibility which derive entirely from the matrix method and which do not relate to the presence of incipient phase transitions.

As n becomes large we should expect the weight of these objections to decrease, in the sense that all the maxima discussed in (i) and (ii) would tend to coalesce and those of (iii) would tend to disappear. If, as in our case, investigations are possible only for small n, then only general qualitative predictions of the phase transitions can be given. To

distinguish between genuine incipient phase transitions and spurious maxima and to predict the order of phase transitions we must rely on the results of approximation methods. Ree and Chesnut (1966), Bellemans and Nigam (1967), Orban and Bellemans (1968), Orban *et al* (1968), Runnels and Combs (1966) and Runnels *et al* (1967) chose to locate phase transitions by plotting a function of the form (4.4), with $i = 0, j = 1$ and $k = 2$, against μ'/T'. Comparisons by Bellemans and Nigam (1967) with series and closed-form approximations yielded good qualitative agreement. We have chosen to plot a function of the form (4.4), with $i = j = 0$ and $k = 2$, against μ'. For plots along an isotherm this is of course equivalent to the choice of the above mentioned authors.

5. Boundary properties

The effect of a boundary on the structure of the assembly can be measured in a large number of different ways. One of the most concise parameters is that of Bell and Salt (1973) who calculated the difference, in the thermodynamic limit, between the number of pairs of elements with particular occupations on an open chain of N elements and on a chain for which the first and $(N+1)$th elements coincide. The difficulty of this parameter for us is that it involves calculation of all the eigenvectors of $\mathbf{V}$. This, at least for $n = 2$, where $\mathbf{V}$ is 81×81, would need a considerable expenditure of computer time. We have chosen rather to use parameters which can be represented entirely in terms of the elements of the probability vector $\boldsymbol{p}(r)$.

In terms of the $2n$-dimensional occupation vector $\boldsymbol{\eta} = (s_{2n}, s_{2n-1}, \ldots, s_1)$ we define the function

$$\Delta(\boldsymbol{\eta}; s, j) = \begin{cases} 1 & \text{if } s_j = s \\ 0 & \text{otherwise.} \end{cases} \tag{5.1}$$

The probability $p_m(r)$ that the rth site in the first row of the lattice is occupied by a monomeric molecule is given by

$$p_m(1) = \sum_{\boldsymbol{\eta}} p_{\eta}(1)\Delta(\boldsymbol{\eta}; -1, 1)(1-\Delta(\boldsymbol{\eta}; +1, 2))(1-\Delta(\boldsymbol{\eta}; +1, 2n))$$

$$+ \sum_{\boldsymbol{\eta}, \boldsymbol{\zeta}} p_{\eta}(1)\Delta(\boldsymbol{\eta}; +1, 1)p_{\zeta}(2)(1-\Delta(\boldsymbol{\zeta}; -1, 1)), \tag{5.2a}$$

for $r = 1$ and

$$p_m(r) = \sum_{\boldsymbol{\xi}, \boldsymbol{\eta}} p_{\xi}(r-1)(1-\Delta(\boldsymbol{\xi}; +1, 1))p_{\eta}(r)\Delta(\boldsymbol{\eta}; -1, 1)(1-\Delta(\boldsymbol{\eta}; +1, 2))$$

$$\times(1-\Delta(\boldsymbol{\eta}; +1, 2n)) + \sum_{\boldsymbol{\xi}, \boldsymbol{\eta}, \boldsymbol{\zeta}} p_{\xi}(r-1)(1-\Delta(\boldsymbol{\xi}; -1, 2))(1-\Delta(\boldsymbol{\xi}; -1, 2n))$$

$$\times p_{\eta}(r)\Delta(\boldsymbol{\eta}; +1, 1)p_{\zeta}(r+1)(1-\Delta(\boldsymbol{\zeta}; -1, 1)) \tag{5.2b}$$

for $r > 1$. The local number density $\rho_L(r)$ on the rth element of the lattice is given by

$$\rho_L(r) = \frac{1}{2n}\sum_{\boldsymbol{\eta}} p_{\eta}(r) \sum_{j=1}^{2n} \zeta_j^2 \tag{5.3}$$

for $r \geqslant 1$ and

$$\lim_{r\to\infty} \rho_L(r) \equiv \rho_L(\infty) = \rho \tag{5.4}$$

where ρ is the bulk number density given by equations (4.1).

We use the parameters $p_m(r)$ and $\rho_L(r)$ to measure the effects of the boundary on the structure of the assembly.

6. Results and discussion

In all our calculations we choose the energy ratio $(\epsilon/w) = 0{\cdot}25$, this being the value for which the properties of the model, as investigated by the first-order approximation of Lavis (1973) are most water-like. In order to obtain numerical results for this problem we need to solve the eigen-problem for the matrix **V**. For the two cases considered, $n = 1$ and $n = 2$, we make full use of the symmetry properties of the matrix which are represented by equations (3.4). These properties allow a considerable simplification of the computational work†.

The pressure in the system is given, as a function of reduced temperature and chemical potential, by equation (3.17*a*) and we obtain the bulk number density ρ by five-point numerical differentiation according to equation (4.1*a*). As a check on numerical accuracy we also obtained the number density from the principal eigenvector using equations (3.14*b*) and (4.1*b*). These results gave seven-figure agreement in every case. This also gives an indication of the accuracy of the numerical differentiation involved in the determination of $\rho^2\kappa'_T$ according to equation (4.3). The functions P', ρ, $\rho^2\kappa'_T$ and $|h_2|^n$ are plotted in figures 2 and 3, for $n = 1$ and $n = 2$ respectively, against the reduced chemical potential μ' along the isotherm $T' = 0{\cdot}15$. These are just two of a whole set of graphs which were drawn for varying values of the temperature. From these graphs the isobars given in figure 4 were constructed. It would of course have been possible to obtain these isobars by direct numerical calculation. This would have involved the use of a root-finding subroutine to determine the value of μ' corresponding to a particular value of x_1 and of T'. Such calculations would have consumed large amounts of computing time, yielding in return a degree of accuracy which could not have been represented in the final graphs. The isobars in figure 4, like those of Bell and Salt (1973) exhibit the characteristic water-like density maximum below the reduced separation pressure $P'_0 = 0{\cdot}25$. They also show, although of course not exhibiting a phase transition, a resemblance to the isobars of Lavis (1973). As in the work of Bell and Lavis (1970b), this density maximum has been achieved entirely by the effect of molecular bonding on the short-range ordering on the lattice. We may tentatively infer that this kind of mechanism is responsible for the parallel behaviour in liquid water.

In figure 5 we have plotted the maxima of $\rho^2\kappa'_T$, as a function of μ' along isotherms, in the (P', T') plane. A trajectory of maxima, for both $n = 1$ and $n = 2$, leaves the point $P' = 0$, $T' = 0$ and follows fairly closely the corresponding phase transition curve of the first-order approximation of Lavis (1973). These maxima are, for low temperatures, extremely steep (see figures 2 and 3) and for all temperatures they are steeper for $n = 2$ than for $n = 1$. It is not unreasonable to suppose that they correspond to a genuine incipient phase transition which in the limit as n tends to infinity would give the first-order phase transition to or from the low-density gaseous state. Support for this

† The details of our method are contained in an unpublished appendix.

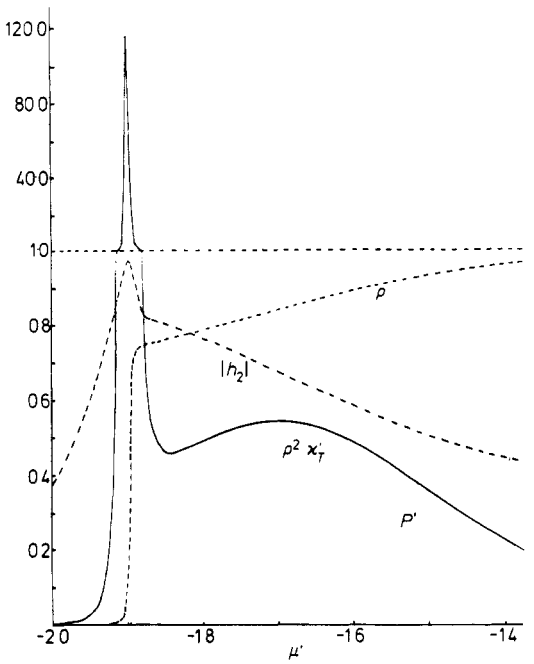

Figure 2. Curves of P', ρ, $\rho^2\kappa'_T$ and $|h_2|$ plotted against μ' along the isotherm $T' = 0{\cdot}15$ for $n = 1$. The scale of the vertical axis changes at the value $1{\cdot}0$.

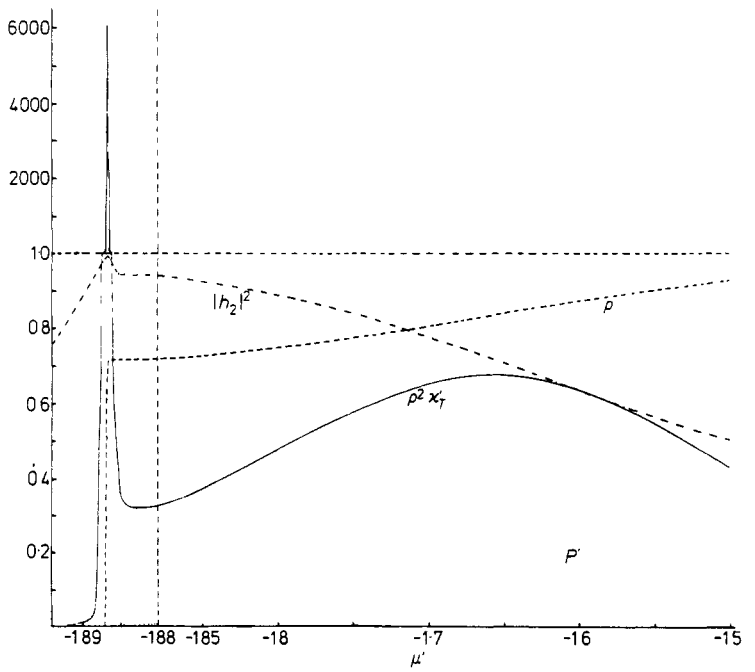

Figure 3. Curves of P', ρ, $\rho^2\kappa'_T$ and $|h_2|^2$ plotted against μ' along the isotherm $T' = 0{\cdot}15$ for $n = 2$. The scale of the vertical axis changes at the value $1{\cdot}0$ and the horizontal axis at $-1{\cdot}88$.

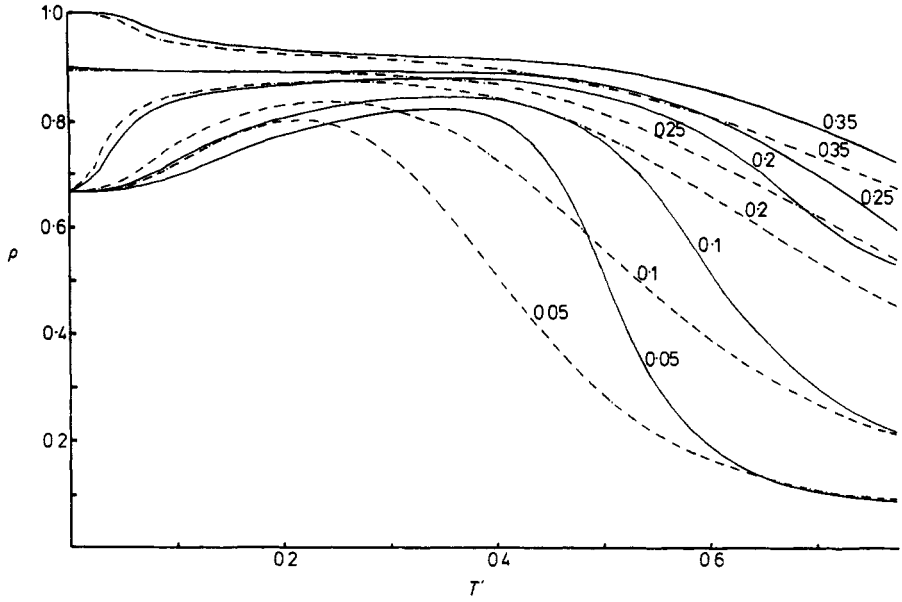

Figure 4. Isobars for $n = 1$ (chain curves) and $n = 2$ (full curves) plotted in the density–temperature plane. The curves are labelled with their values of P'.

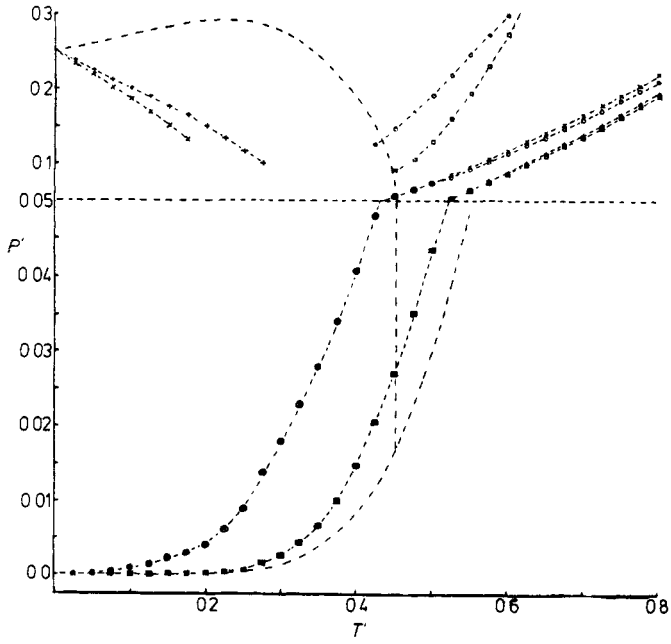

Figure 5. Trajectories of the maxima of $\rho^2\kappa'_T$ and $|h_2|^n$. For $n = 1$ the maxima of $\rho^2\kappa'_T$ are denoted by × and the maxima of $|h_2|$ by ○. For $n = 2$ the maxima of $\rho^2\kappa'_T$ are denoted by + and the maxima of $|h_2|^2$ by □. The chain curve represents the phase transition curve of Lavis (1973). The scale of the vertical axis changes at 0·05.

conjecture is given by figure 4, where we see that, for low pressures, the isobaric coefficient of thermal expansion $-\rho^{-1}(\partial\rho/\partial T)_P$ attains larger values for $n = 2$ than for $n = 1$ in the same temperature range. For T' less than about 0·275 for $n = 2$ and 0·175 for $n = 1$ there is a second maximum in $\rho^2\kappa'_T$. The trajectory of these maxima, as T' increases from zero, leaves the point $P' = P'_0$ as does the corresponding phase transition curve for the first-order approximation. Since the pressure P'_0 is the pressure which separates the stable equilibrium ranges of the close-packed and honeycomb arrangements of molecules at zero temperature (see § 2) it is strongly suggested that this curve corresponds to the first-order transition to or from the solid phase. Although the maximum in this case is much shallower than that which occurs at the lower pressure, it does become steeper for increasing n (cf figures 2 and 3). It is unfortunate that this second maximum disappears before it can coalesce with the lower pressure maximum in a triple point, but it is reasonable to suppose that, if n could be extended to higher values, a triple point could be obtained.

In figure 5 we have also represented the trajectories of the maximum of $|h_2|^n$ for $n = 1$ and $n = 2$. This maximum approaches very closely its degeneracy value of unity and the trajectories follow those of $\rho^2\kappa'_T$ up to high temperatures where a slight divergence is detected. Around these temperatures a second maximum for $n = 1$ and $n = 2$ appears. Since this is extremely shallow it is probably of no physical significance. Of more significance, in view of the discussion in § 4, is the result that $|h_2|^n$ drops in value quite steeply for values of μ' below the lower maximum of $\rho^2\kappa'_T$ and, as μ' increases, it again appears to tend to zero (see figures 2 and 3). Since the range of μ' between the two maxima of $\rho^2\kappa'_T$ will, in the two-dimensionally infinite system, correspond to the long-range ordered solid phase, it must be in this range that a function $f(\mu') \neq 0$, and given by (4.2), will exist.

In dealing with the boundary properties of the system we choose two types of interaction between the first element of the lattice and the boundary:

(a) *The fully-bonded boundary*, where $E_\eta^{(L)} = 0$ if $\boldsymbol{\eta}$ is the occupational state representing a bonded ring of sites and $E^{(L)} = \infty$ otherwise.
(b) *The indifferent boundary*, where $E_\eta^{(L)} = 0$ for all occupational states $\boldsymbol{\eta}$.

Since the successive occupations of elements of the lattice are, in the thermodynamic limit, given by a homogeneous Markov chain the boundary can produce no long-range disturbance in the assembly. The effects of the boundary must decay as penetration into the bulk of the lattice deepens. The purpose of our calculations is to discover the way in which this decay occurs and the effect upon it of different types of boundary and different values of the temperature and chemical potential. Computations were performed for two values, $T' = 0{\cdot}15$ and 0·6, of the temperature and two values, $\mu' = -1{\cdot}8$ and $-1{\cdot}4$, of the chemical potential. In figure 6, $p_m(r)$ and $\rho_L(r)$ are shown for $n = 2$, $T' = 0{\cdot}15$ and $\mu' = -1{\cdot}8$ with a fully-bonded boundary. Of the cases considered this is the one for which boundary effects are most marked. This is to be expected since, at low temperatures, short-range ordering, in terms of bonded clusters of molecules, will be most evident and the chemical potential $\mu' = -1{\cdot}8$ fall in the range between the two maxima of the compressibility (see figure 3) and will therefore correspond most nearly to the occurrence of a solid phase.

The most interesting feature of figure 6 is the three-element damped periodicity of the chains. This again is easily understood since the honeycomb bonded molecular structure has a periodicity of three with respect to the elements of the lattice (see figure

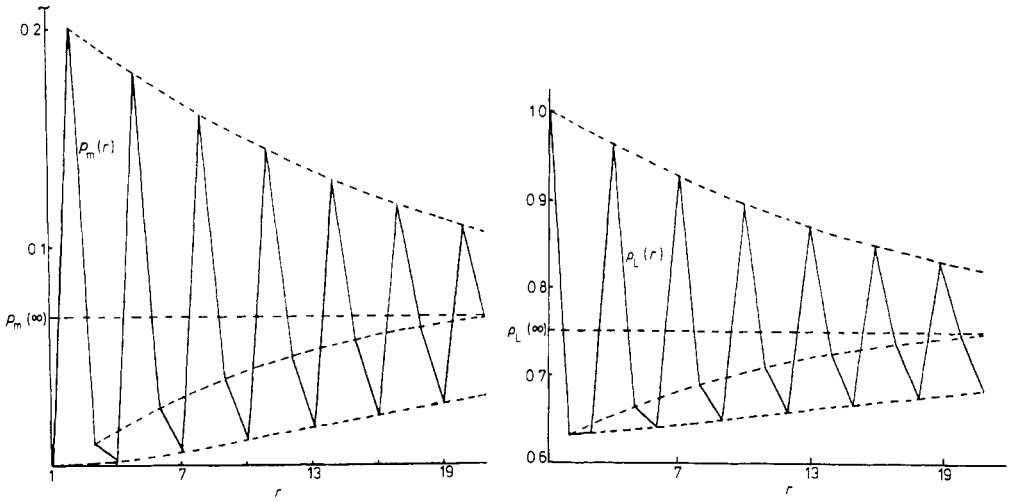

Figure 6. Values of $p_m(r)$ and $\rho_L(r)$ for a fully-bonded boundary with $n = 2$. The value of the reduced temperature is 0·15 and of the reduced chemical potential is $-1{\cdot}8$.

1). Since no long-range ordering occurs in the assembly, the bulk values $p_m(\infty)$ and $\rho_L(\infty) = \rho$ of the monomer probability and the local density can be viewed as averages over the period of the short-range ordering. The effect of a fully-bonded boundary is to impose a particular phase on the periodicity of the Markov chain. The decay in amplitude of the variations in $p_m(r)$ and $\rho_L(r)$ as we proceed along the chain can be understood as a process of phase-mixing which ultimately produces the average values associated with the bulk of the assembly. It is interesting to note that the quantity $\rho_L(r)/\rho$ (obtained from figure 6 by scaling the vertical axis) has a behaviour very similar to that of the radial distribution function for liquid water (see Eisenberg and Kauzmann 1969, p 157). Since the local density is calculated over an element of the lattice and measured in one dimension, there can of course be no exact identification of these two quantities. It can nevertheless be argued that $\rho_L(r)/\rho$ is the quantity most nearly equivalent to the radial distribution function for our model. The fact that we are measuring from a boundary is not important here. If we were to close the lattice by bringing the first and $(N+1)$th elements together on the surface of a torus of infinite radius, then a fully-bonded ring of molecules on the first (or any other) element would have exactly the effect in both directions along the torus as does our boundary element.

While, as we have indicated, the depth of penetration of boundary effects is greater for the lower of our two chosen temperatures, the distinction between choosing the fully-bonded or indifferent boundary shows up most clearly for the higher temperature. Since the effect of the indifferent boundary is exactly that which would be produced if a completely vacant lattice element were situated to the left of the first element, it is not surprising that there is a strong tendency for the first element to be fully-bonded. This tendency is reduced by thermal agitation as the temperature is increased thereby producing a clearer differentiation between the indifferent and fully-bonded boundary. Because of the averaging represented by $p_m(\infty)$ and $\rho_L(\infty)$ it is, in some ways, more reasonable to investigate boundary effects by comparing these quantities with similar averages taken over elements of the lattice near to the boundary. We define the relative

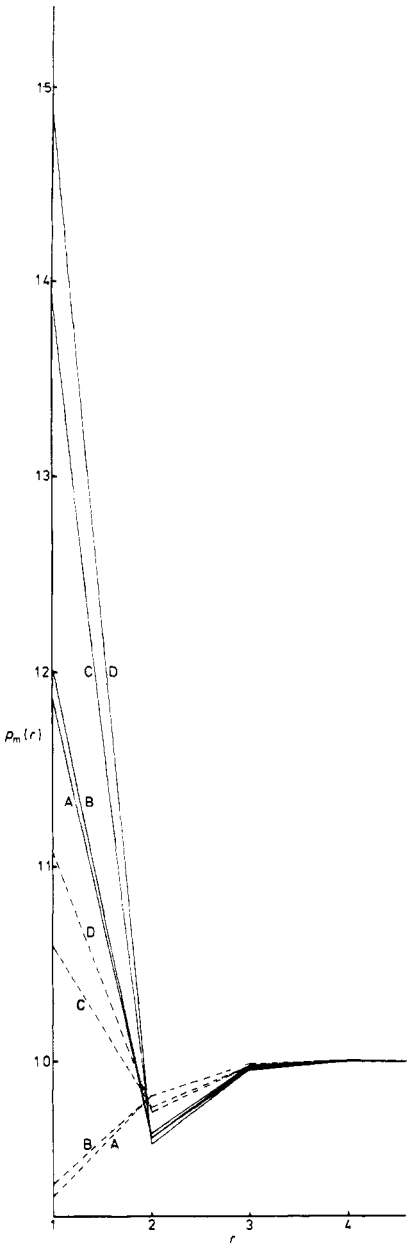

Figure 7. Values of $\tilde{\rho}_m(r)$ for $T' = 0{\cdot}6$. Full curves represent the fully-bonded boundary and chain curves the indifferent boundary with: A, $\mu' = -1{\cdot}8$, $n = 1$; B, $\mu' = -1{\cdot}4$, $n = 1$; C, $\mu' = -1{\cdot}8$, $n = 2$; D, $\mu' = -1{\cdot}4$, $n = 2$.

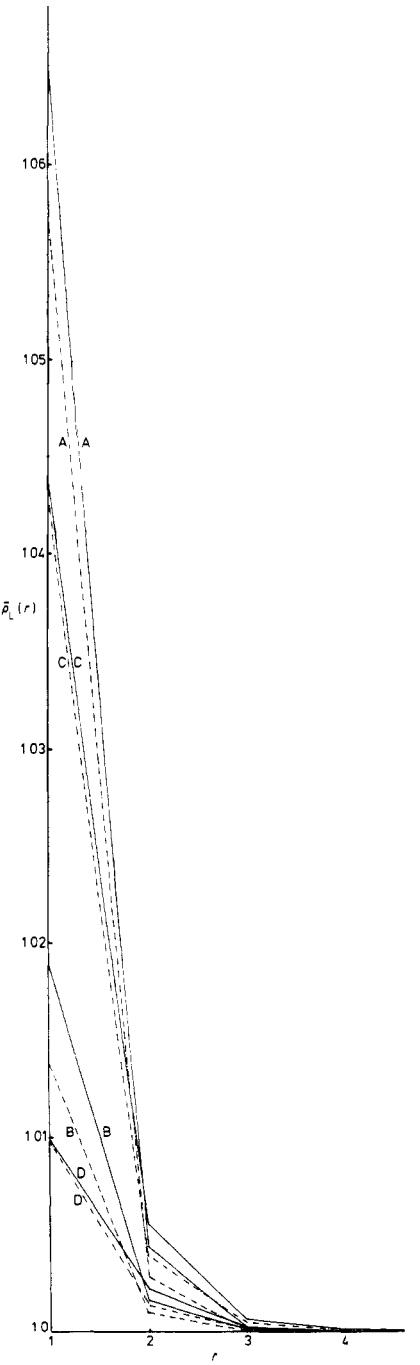

Figure 8. Values of $\tilde{\rho}_L(r)$ for $T' = 0{\cdot}6$. Full curves represent the fully-bonded boundary and chain curves the indifferent boundary with: (A) $\mu' = -1{\cdot}8$, $n = 1$; (B) $\mu' = -1{\cdot}4$, $n = 1$; (C) $\mu' = -1{\cdot}8$, $n = 2$; (D) $\mu' = -1{\cdot}4$, $n = 2$.

period averages of $p_m(r)$ and $\rho_L(r)$ by

$$\tilde{p}_m(r) = \frac{p_m(3r-2)+p_m(3r-1)+p_m(3r)}{3p_m(\infty)} \tag{6.1a}$$

and

$$\tilde{\rho}_L(r) = \frac{\rho_L(3r-2)+\rho_L(3r-1)+\rho_L(3r)}{3\rho_L(\infty)} \tag{6.1b}$$

respectively, where

$$\lim_{r\to\infty} \tilde{p}_m(r) = 1{\cdot}0 \qquad \text{and} \qquad \lim_{r\to\infty} \tilde{\rho}_L(r) = 1{\cdot}0.$$

We investigated the lattice to the depth of fifty-three elements. By this stage, in all cases except $T' = 0{\cdot}15$, $\mu' = -1{\cdot}8$, $n = 2$, the parameters had to the fourth decimal place attained their limiting values. Even in this one case the limiting values had been attained to the second decimal place. The difference in behaviour associated with the two choices of boundary disappeared very close to the boundary and, in the case of the lower temperature, before the effect of the disturbance itself disappeared. In all cases the disturbance penetrated to a greater depth for $n = 2$ than for $n = 1$. This is to be expected because of the greater structure-creating possibilities afforded by the larger value of n. In figures 7 and 8 our results are displayed for the temperature $T' = 0{\cdot}6$. The general conclusion to be drawn from our work is that the model is in agreement with the experimental work of Clifford *et al* (1970) and the theoretical studies of Bell and Salt (1973) in showing that boundary effects cause only a short-range disturbance on the structure of the system.

In the absence of an exact solution to the two-dimensionally infinite system, the best we are able to do is to approach the problem, either by an approximation method, as in the investigation of bulk properties by Lavis (1973), or by solving exactly for a lattice with a finite number of rows, as in the present work. Any predictions about the properties of the two-dimensionally infinite system made on this basis are necessarily speculative.

Appendix: Symmetry properties

The symmetry of an element of the lattice is represented by the dihedral group $\mathscr{D}_{nd}$. This group consists of:

(i) The n rotations $\{I, C_n^{(1)}, \ldots, C_n^{(n-1)}\}$, where $C_n^{(s)}$ is a rotation through an angle of $2\pi s/n$ radians about the axis of the cylinder and $I = C_n^{(n)}$ is the identity element.

(ii) The n reflections $\{\sigma_1, \ldots, \sigma_n\}$, where σ_s is a reflection through the plane containing the axis of the cylinder and the row with index s.

(iii) The n rotations $\{U_2^{(1)}, \ldots, U_2^{(n)}\}$, where $U_2^{(s)}$ is a rotation through an angle of π radians about the axis which passes through the points P_s and P_{n+s}.

(iv) The n improper rotations $\{S_{2n}^{(1)}, S_{2n}^{(3)}, \ldots, S_{2n}^{(2n-1)}\}$ where $S_{2n}^{(2s-1)}$ is a rotation through an angle of $(2s-1)\pi/n$ radians about the axis of the cylinder together with a reflection through the plane containing the points $P_1, P_2, \ldots, P_{2n}$.

The multiplication table for this group is given in an unpublished appendix.

The rotational subgroup $\mathscr{C}_n$ of $\mathscr{D}_{nd}$ contains the rotations $\{I, C_n^{(1)}, \ldots, C_n^{(n-1)}\}$ and the subgroup $\mathscr{C}_{nv}$ contains these rotations and the reflections $\{\sigma_1, \ldots, \sigma_n\}$.

The importance of these group operations for our model becomes clear if we make the following observations.

(a) An occupational state $\boldsymbol{\eta}$ of an element of the lattice will, under any operation of $\mathscr{D}_{nd}$, map into another occupational state $\boldsymbol{\eta}'$ with

$$E_{\eta} = E_{\eta'} \tag{A.1a}$$

$$\mu_{\eta} = \mu_{\eta'}. \tag{A.1b}$$

(b) For two neighbouring occupational states $\boldsymbol{\eta}$ and $\boldsymbol{\xi}$ which map into neighbouring occupational states $\boldsymbol{\eta}'$ and $\boldsymbol{\xi}'$

$$E_{\eta\xi} = E_{\eta'\xi'} \tag{A.2a}$$

if the operator is a member of $\mathscr{C}_{nv}$ and

$$E_{\eta\xi} = E_{\xi'\eta'} \tag{A.2b}$$

if the operator is one of the rotations $\{U_2^{(1)}, \ldots, U_2^{(n)}\}$.

We order the occupational states according to their symmetry properties, collecting together all occupations which permute among themselves under the operations of $\mathscr{D}_{nd}$, and within these sets we form subsets which permute under the operations of $\mathscr{C}_{nv}$ and $\mathscr{C}_n$. If the occupational state represented by the $2n$-dimensional vector $\boldsymbol{\eta}$ appears as the rth state in this ordering we now represent it alternatively by the 3^{2n}-dimensional vector $\hat{\boldsymbol{\imath}}_{\eta}$ which has zeros in all entries except the rth which is unity. The elements of $\mathscr{D}_{nd}$ have a 3^{2n}-dimensional representation R which represents the operations of $\mathscr{D}_{nd}$ on the occupational states of the system. The ordering of occupational states and the corresponding representations for $n = 1$ and $n = 2$ are given in an unpublished appendix.

Acknowledgments

I wish to thank Professor G M Bell and Mr L Dunne for valuable discussions. Computation was performed on the CDC6600 computer of the University of London. Advice on computation was given by Mrs Jill Skok and Miss Lynda Brookes.

References

Bell G M 1969 *J. Math. Phys.* **10** 1753–60
—— 1972 *J. Phys. C: Solid St. Phys.* **5** 889–905
Bell G M and Lavis D A 1970a *J. Phys. A: Gen. Phys.* **3** 427–41
—— 1970b *J. Phys. A: Gen. Phys.* **3** 568–81
Bell G M and Sallouta H 1975 *Molec. Phys.* **29** 1621–37
Bell G M and Salt D W 1973 *Molec. Phys.* **26** 887–903
—— 1976 *J. Chem. Soc., Faraday Trans.* II **72** 76–86
Bellemans A and Nigam R K 1967 *J. Chem. Phys.* **46** 2922–35
Bernal J D and Fowler R H 1933 *J. Chem. Phys.* **1** 515–48
Clifford J, Oakes J and Tiddy G J T 1970 *Spec. Disc. Faraday Soc.* **1** 1972
Domb C 1960 *Adv. Phys.* **9** 149–361
Eisenberg D and Kauzmann W 1969 *The Structure and Properties of Water* (London: Oxford University Press)
Fletcher N A 1970 *The Chemical Physics of Ice* (Cambridge: Cambridge University Press)
Gantmacher F R 1959 *Applications of the Theory of Matrices* (London: Interscience)
Lavis D A 1973 *J. Phys. C: Solid St. Phys.* **6** 1530–45
—— 1975 *J. Phys. A: Gen. Phys.* **8** 1933–51

Orban J and Bellemans A 1968 *J. Chem. Phys.* **49** 363–70
Orban J, van Craen J and Bellemans A 1968 *J. Chem. Phys.* **49** 1778–83
Parzen E 1960 *Modern Probability Theory and Its Applications* (New York: John Wiley)
Perram J W 1971 *Molec. Phys.* **20** 1077–85
Perram J W and Levine S 1974 *Adv. Molec. Relax. Process.* **6** 85–122
Ree F H and Chesnut D A 1966 *J. Chem. Phys.* **45** 3983–4003
Runnels L K and Combs L L 1966 *J. Chem. Phys.* **45** 2482–92
Runnels L K, Combs L L and Salvant J P 1967 *J. Chem. Phys.* **47** 4015–20
Watson P G 1972 *Phase Transitions and Critical Phenomena*, vol. 2 eds C Domb and M S Green (London: Academic Press)